Journal Pre-proof

Accuracy and precision of the measurement of liner orientation of dual mobility cup total hip arthroplasty using ultrasound imaging

Louis Riglet , Anthony Viste , Tristan De Leissegue , Alexandre Naaim , Hervé Liebgott , Raphaël Dumas , Michel Henri Fessy , Laure-Lise Gras

PII: S1350-4533(22)00125-4
DOI: https://doi.org/10.1016/j.medengphy.2022.103877
Reference: JJBE 103877

To appear in: *Medical Engineering and Physics*

Received date: 27 January 2022
Revised date: 18 July 2022
Accepted date: 22 August 2022

Please cite this article as: Louis Riglet , Anthony Viste , Tristan De Leissegue , Alexandre Naaim , Hervé Liebgott , Raphaël Dumas , Michel Henri Fessy , Laure-Lise Gras , Accuracy and precision of the measurement of liner orientation of dual mobility cup total hip arthroplasty using ultrasound imaging, *Medical Engineering and Physics* (2022), doi: https://doi.org/10.1016/j.medengphy.2022.103877

| Technical Note

Accuracy and precision of the measurement of liner orientation of dual mobility cup total hip arthroplasty using ultrasound imaging

Louis Riglet[1], Anthony Viste[1,2], Tristan De Leissegue[2], Alexandre Naaim[1], Hervé Liebgott[3], Raphaël Dumas[1], Michel Henri Fessy[1,2], and Laure-Lise Gras[1,*]

[1]Univ Lyon, Univ Gustave Eiffel, Univ Claude Bernard Lyon 1, LBMC UMR_T9406, F69622, Lyon, France

[2]Hospices Civils de Lyon, Hôpital Lyon Sud, Service de Chirurgie Orthopédique, 165 Chemin du Grand Revoyet, 69495 Pierre Benite Cedex, France

[3]CREATIS, Univ Lyon, INSA Lyon, UCBL, UJM Saint-Étienne, CNRS UMR 5220, Inserm U1294, Lyon, France

[*]**Corresponding author:** Laure-Lise Gras, Laboratoire de Biomécanique et Mécanique des Chocs, Université Gustave Eiffel, 25 avenue François Mitterrand, Case24, Cité des mobilités, F-69675 Bron, France, Email: laure-lise.gras@univ-lyon1.fr

Highlights

- In vivo motion of the polyethylene liner of dual mobility cup is unclear
- Liner position is studied when DMC is submerged and implanted ex vivo
- Liner position is calculated using motion analysis and 3D ultrasound imaging
- The study demonstrated the feasibility to analyse liners using ultrasound imaging

Abstract

The Dual Mobility Cup (DMC) was created in 1974 to prevent dislocation and decrease wear. However, the movement of the polyethylene liner *in vivo* remains unclear. The aims of this study were to visualise liner positions and quantify the accuracy of the liner plane orientation for static positions, using ultrasound imaging. DMC reconstruction and angle between cup and liner were evaluated on isolated submerged DMCs by comparing 3D laser scans and ultrasound imaging. Moreover, the abduction and anteversion angles of the liner plane relative to the pelvis orientation were calculated via combined motion analysis and 3D ultrasound imaging on four fresh post-mortem human subjects with implanted DMC. On submerged DMC, the mean angle error between ultrasound imaging and 3D scan was 1.2°. In cadaveric experiments, intra-operator repeatability proved satisfactory, with low range value (lower than 2°) and standard deviation (lower than 1°). The study demonstrates the feasibility of measuring liner orientation on submerged and *ex vivo* experiments using ultrasound imaging, and is a first step towards *in vivo* analysis of DMC movement.

Keywords: Dual mobility cup, *ex vivo* experiment, ultrasound imaging, motion analysis, biomechanics

1. Introduction

Total Hip Arthroplasty (THA) is one of the most successful orthopaedic surgical procedures [1]. While numerous advances have led to improved patient satisfaction and implant longevity, prosthesis dislocation and wear remain major causes of failure [2,3]. The Dual Mobility Cup (DMC), developed in 1974 by G. Bousquet and A. Rambert [4], relies on the "Low Friction" principle defined by Charnley [5] and on the McKee-Farrar concept [6]. The device is composed of two joints: a large one between the metal shell and the polyethylene liner, and a small one between the femoral head and the polyethylene liner. Compared to the standard prosthesis, its design presents the advantages of restoring hip range of motion, decreasing wear, and increasing implant stability [6]. Historically, orthopaedic surgeons saved this concept for patients with a high risk of dislocation: elderly patients, patients with neurological pathologies, etc. [1,6]. More recent clinical studies have shown good results regarding DMC-THA stability [1,7–10], and its use has been extended to unselected population [9].

However, its biomechanical behaviour remains poorly understood [13] due to the lack of *in vivo* assessment of the prosthesis, especially the liner movement [14,15]. The amplitude of liner movement (together with contact force) is of paramount importance to appropriately estimate wear on the implant [16,17]. In theory, the small joint moves during low range of motion movements like walking. The large joint moves when a contact occurs between stem and liner, during large range of motion movements like climbing, descending stairs, etc. [18–20].

Experimentally, liner mobility has been analysed in load cases representative of daily activity via an industrial robot and stereo camera system [21]. Using a concentric tripolar system, Fabry et al. [21] showed that the dynamic behaviour of the liner was controlled by the stem movement. In fact, intermediate motion was shown to appear primarily after stem contact. Cadaveric experiments carried out [15,22,23] to visualise and quantify impingement between soft tissues and liners through visual observation and fluoroscopic imaging revealed that liner motion was modified by iliopsoas tendon impingement at low flexion angles. Employing finite element analysis, Zumbrunn et al. [23] showed that tendon-liner contact pressure and tendon stresses were reduced by using an anatomical contoured dual mobility liner. Moreover, Fessy et al. [14] reported for the first time, from an original case report, *in vivo* impingement between the iliopsoas tendon and the liner, describing it based on ultrasound imaging and arthro-CT-scan.

The potential of ultrasound imaging to measure liner position was demonstrated by Desmarchelier et al. [24,25] via experiments involving ultrasound acquisitions on submerged DMC-THA. Seeking a method of increasing the *in vivo* understanding of this prosthesis, they measured the angles between the opening planes of the liner and the metal shell and compared them to the angles obtained using a 3D laser scan. An average deviation of 2.2° was revealed for static DMC positions. Since the limited accuracy obtained with a submerged and isolated DMC-THA, added to the time-consuming data analysis procedure, could make ultrasound unattractive for the assessment of liner movement, we investigated possible improvements.

Extending the work of Desmarchelier et al. [24], we propose a semi-automatic method of visualising and calculating the liner positions of DMC-THA via ultrasound imaging. Our first objective was to assess the accuracy of the method by comparing the liner plane orientation measured with ultrasound imaging to that obtained with a 3D laser scan. This was done *in vitro* on a submerged DMC-THA in static positions. Our second objective was to evaluate the feasibility and repeatability of the methodology, this time during *ex vivo* experiments carried out on four post-mortem human subjects (PMHS). The liner position in static supine position was assessed by data fusion of ultrasound images and motion analysis data.

2. Materials and methods

1. *Ultrasound imaging analysis*

To evaluate DMC liner positions, ultrasound volumes were acquired with a 3D probe (SuperLinear™ Volumetric SLV16-5) connected to the ultrasound Aixplorer® system from Supersonic Imagine® (Figure 1). The ultrasound acquisition takes 5 seconds and provides a 3D volume (slice ~ each 0.1 mm, size volume ~ 45 × 45 × 40 mm^3). With a single acquisition volume, part of the DMC can be visualised and acquired, allowing its 3D reconstruction. After acquisition, ultrasound volume data were imported in 3D Slicer software, and metal shell, polyethylene liner, shell plane and liner plane were segmented using a threshold on the grey-scale level of the B-mode image (Figure 2). Threshold values were chosen empirically so as to obtain the largest point clouds representing the real DMC components in the STL segment export. These values also depend on image characteristics (voxel intensities, component sizes, etc.). Based on the component diameters, an Iterative Closest Point (ICP) method [26] was used to fit spheres to the 3D point clouds of the metal shell and liner. A best-fit of a plane on the liner and on the metal shell plane 3D point clouds was carried out using the least squares method. Then, using this fitting was used to calculate the angle between the two planes (Figure 1) [27]. This method was applied to the submerged DMC-THA; alternatively, for the images obtained *ex vivo*, where the metal shell plane cannot be segmented because of its position in the acetabulum (metal shell hidden by pelvis bone and therefore its plane not visible on US images), the abduction and anteversion angles of the liner plane were calculated relative to the pelvis. The pelvis coordinate system was defined in accordance with the International Society of Biomechanics recommendations [28]. Post processing was performed using a custom-made script in Matlab (MathWorks®).

2. *Submerged dual mobility cup*

A Novae Sunfit TH 47/28 DMC (Serf®, Décines-Charpieu, France) of concentric design was placed manually in specific positions using a fixation paste. A 3D laser scan (Nikon®) of the DMC was performed (Figure 1). Without moving any components of the DMC-THA, the hip prosthesis was submerged in water and an ultrasound acquisition performed (Figure 1). This protocol was repeated for 22 DMC-THA positions, corresponding to a range of liner orientations with respect to the metal shell position (from 4.0° to 73.2°).

Offsets, i.e. the distance between centres of prosthesis elements, which should be zero because of the DMC concentric design, and liner plane orientation with respect to metal shell plane were calculated for each imaging system. Offset and angle errors, i.e. the difference between US and scan measurements, were calculated for each liner position.

3. *Implanted dual mobility cup*

Four un-embalmed and frozen PMHS from the Department of Anatomy of the University of Rockefeller (DAUR), Lyon, France, were instrumented with DMC-THA and prepared for motion analysis (**Error! Reference source not found.**). These subjects were on average 89.5 years old (SD: 10.5 years old), with a height of 160 cm (SD: 10.2 cm) and a weight of 61 kg (SD: 24.1 kg). Each frozen PMHS was thawed at room temperature three days before testing. During tests, the body was placed on a table in a supine position. Tests were performed at ambient temperature. The use of PMHS was approved by the institutional review board, and these experiments were performed under appropriate health and safety conditions.

Each hip was instrumented with a DMC-THA by experienced orthopaedic surgeons using an anterior approach. DMC-THA size was determined before surgery. Acetabular and femoral preparations were carried out in accordance with the guidelines provided by the manufacturer Serf. In order to ensure the propagation of ultrasound waves without air, the hip was filled with Aquasonic® 100 ultrasound transmission gel. Then, the arthrotomy was closed and an X-ray taken to check DMC-THA position. For motion analysis, six intracortical pins with four reflective-marker tripods (10 mm diameter) were fixed in the pelvis, in both femurs and in both tibias (Figure 4). The tripods were placed in such a way as to avoid contact with the operator and leg segments during the experiment.

Motion analysis was performed using the Optitrack system with 10 cameras (frame rate of 200Hz) oriented such that the tripod markers were visible during the tests (Figure 4). The volume of interest being approximately $2 \times 1.5 \times 2$ m^3, marker position can be considered accurate to less than 1mm, according to manufacturer data. Intracortical pins fixed in the lower limbs were used to define technical coordinate systems for each segment. Anatomical coordinate systems were based on landmark positions relative to the intracortical pins measured using a calibrated tip. As with the pelvis, femur and tibia/fibula landmarks were defined in accordance with the International Society of Biomechanics recommendations [29]. However, with the PMHS supine on the table, posterior superior iliac spine positions were inaccessible. We assumed that the mid-point of the left and right posterior superior iliac spines and the mid-point of the left and right anterior superior iliac spines lie on the same vertical line. Data processing was carried out with Qualisys Tracker Manager software (version 2020.3; Qualisys) and using a custom-made script in Matlab (MathWorks®).

One rigid tripod was fixed on the 3D ultrasound probe support (used to protect the ultrasound probe) to register image volume with motion analysis data. Wave propagation celerity was set at 1540 $m.s^{-1}$. Depending on the corpulence of the subject, depth and focal zone were adjusted during experiments to obtain the best-defined images (depth between 36.5 mm and 62.7 mm, focal zone between [54.5;37.5] mm and [32.5;19.5] mm). To enable ultrasound wave propagation

during acquisitions, ultrasound transmission gel was applied to the 3D ultrasound probe. The ultrasound system was time-synchronized with motion analysis via a pedal sending a rising-edge square signal to both systems. Calibration of the ultrasound probe was performed by measuring the positions of 3 reflective markers both on ultrasound images and in the motion analysis coordinate system.

Data processing was carried out according to the proposed methodology. However, only the liner surface could be segmented, as the head was partially covered by the liner and the metal shell was embedded in the pelvis. Knowing the probe position and the 3D segmentation enabled us to calculate the abduction and anteversion angle of the liner plane relative to the pelvis coordinate system (Figure 5). To quantify repeatability of the ultrasound acquisition procedure, 8 acquisitions of the DMC-THA were performed for each PMHS in a first liner position. Moreover, to quantify intra-operator segmentation repeatability, one ultrasound dataset obtained for each PMHS in a second liner position was processed 8 times. The two liner positions were obtained by applying manually hip motion of large amplitude, whereas the ultrasound was performed with the PMHS back in the same position: straight leg with no internal/external rotation. Moreover, repeatability was quantified by a single operator. Repeatability was assessed as the mean, standard deviation and range of differences between the 8 acquisitions.

3. Results

1. Submerged dual mobility cup

Comparing ultrasound imaging and 3D scan for submerged DMC-THA, mean difference of these imaging systems of the liner orientation with respect to the metal shell is 1.2° (SD: 0.8°). Mean error for the offset between metal shell and liner centres is 0.95 mm (SD: 0.63 mm), between metal shell and femoral head centres is 0.89 mm (SD: 0.87 mm) and between liner and femoral head centres is 0.36 mm (SD: 0.44 mm). With a low correlation coefficient (R^2=0.01, *p-value*=0.62), the error between ultrasound imaging and laser scan is not related to the value of the angle between liner and shell (for graph plot, please see Supplementary material).

2. Implanted dual mobility cup

Ultrasound acquisition procedure repeatability and intra-operator segmentation repeatability of abduction and anteversion angle of the liner plane for PMHS are presented in
. For two PMHS, results are presented for one leg only: in the case of one PMHS, one leg was already instrumented with a Gamma nail, while in the case of the other subject, the DMC-THA was too deeply embedded in the pelvis and could not be seen. Ultrasound acquisition procedure repeatability was not calculated for subject 2020_191_L due to a lack of data. Results show reliable repeatability with a low standard deviation (lower than 1.5°) and range (lower than 3°). The difference between minimum and maximum abduction and anteversion angles shows small difference between PMHS. Moreover, abduction and anteversion range for intra-operator segmentation repeatability is, respectively, lower than 2.5° (mean: 1.8°, SD: 0.6°) and 3° (mean: 1.8°, SD: 0.7°) for all subjects.

4. Discussion

The objective of the present study was to propose and evaluate a semi-automatic method of measuring the liner orientation of DMC-THA using 3D ultrasound imaging.

First, we performed experiments on submerged DMC-THA to demonstrate the feasibility of measuring DMC component position and liner orientation via ultrasound imaging. We obtained a lower liner orientation error between ultrasound imaging and 3D scans than Desmarchelier et al. 2016 [24] (1.2°, SD: 0.8° vs. 2.2°, SD : 2.0°). While that study also performed experiments on submerged DMC-THA, they were processed with a fully manual method and on only five DMC-THA positions. Using ICP, ultrasound data shows a low offset between DMC component centres (less than 1 mm). This error is lower than those found in the literature, where an accuracy of 1 to 3 mm is considered reliable when analysing migration of a prosthetic component on a standard X-ray or a CT scan [30,31].

Secondly, this study assessed the repeatability of liner orientation measurements in *ex vivo* experiments combining motion analysis and ultrasound imaging to measure the abduction and anteversion angles of the liner plane. The repeatability of ultrasound acquisition and intra-operator segmentation were calculated to quantify the precision of the measurement of the liner orientation. Some publications, which study hip prothesis, considered the value of 5° as the threshold value to retain a difference in position of a prosthesis component between two images [18,32–36]. The present method yields good accuracy on liner orientation, with ranges lower than 5°, in agreement with the literature. To our knowledge, this study is the first attempt to use an ultrasound-based system on PMHS to measure liner orientation in DMC-THA. The main advantage of ultrasound imaging is its non-invasive aspect, which explains its frequent use in clinical routine (pregnancy, cardiology, etc.) [37,38]. It enables hip prostheses made of echogenic materials to be observed and differentiated from bone structures [39]. Possible conflicts between THA and the various neighbouring structures (fragments of cement, screws, etc.), the presence of bursitis, fluid collections or even abnormalities on surgical approach can be detected using this non-invasive imaging technique. Unlike other imaging techniques such as mono-plane or bi-plane radiography, ultrasound imaging provides real-time data, is able to detect polyethylene liners and is portable. Moreover, using a 3D ultrasound probe offers a major advantage for further *in vivo* clinical applications. It takes less time to obtain either the full or partial volume than when using a conventional probe that involves acquiring numerous successive images to reconstruct the volume. Furthermore, image reconstruction based on multiple positions of a conventional probe may be less accurate than using a 3D probe with automatic data reconstruction.

A limitation of the *ex vivo* experiments is that because of the metal shell position in the acetabulum, which prevents wave propagation, the shell cannot be visualised from ultrasound data. Therefore, liner orientation is measured relative to the pelvis coordinate system, defined here with intracortical pins and anatomical landmarks. These landmarks are also used during surgery to define the correct shell position, which usually corresponds to an anteversion angle of 15 ±

10 degrees and an abduction angle of 45 ± 10 degrees [40]. Moreover, unlike submerged tests, *ex vivo* experiments make it possible to consider elements surrounding the DMC-THA (soft tissues, bones, etc.), and to obtain images close to those obtained *in vivo* [14].

One issue with the proposed methodology concerns the complexity of ultrasound acquisition, since post processing relies on the quality of the ultrasound images. However, image quality depends on many parameters, including subject corpulence, ultrasound frequency, etc. Due to the different acoustic properties of the materials located in the hip, wave intensity decreases as it propagates through the different soft tissues. Moreover, with a subject presenting a high corpulence, the significant presence of soft tissue requires greater depth of acquisition, which in turn involves low frequencies that lead to low spatial resolution. The right balance between a high frequency, which is desirable to obtain good definition, and a lower frequency, which is required to obtain good penetration, needs to be found. Furthermore, the surface state of the liner plane could be modified so as to be rougher (without altering the mechanical properties). This improvement might enable more ultrasound echoes to be generated and improve liner plane visualisation on ultrasound images.

Moreover, segmentation of DMC components on 3D ultrasound data is complex and not fully automatic, often relying on manual correction. Segmentation in digital image processing is challenging, and various image parameters (noise, contrast, etc.) are known to make it tricky [38,41,42]. In our study, a specific threshold on the grey-scale level of the B-mode image was set to define each different part of the DMC-THA. However, depending on the ultrasound wave incidences, the continuity of liner plane contours is imperfect, making its detection complex. When image quality is poor, the liner plane has to be segmented manually which, while it requires a non-negligible amount of time (5-10 min for one volume), is still less time-consuming than the full manual processing performed by Desmarchelier et al., 2016 [24]. One solution might be to use machine learning, if more data were available; this has been shown to accelerate segmentation for other organs such as the carotid artery, lymph node, etc. [43,44].

Examining only 4 subjects and 6 implanted hip prostheses, this study is subject to the number of samples limitation common to *ex vivo* testing experiments [45]. However, since the aim of the study was to assess the repeatability of liner orientation as well as to validate the experimental method for future *in vivo* tests, the number was considered reasonable and no specific inclusion criteria were applied. Nevertheless, it should be noted that the BMI of these subjects is lower than reported for the population treated with DMC-THA [9,10,46], and their average age is higher [7]. Therefore, the other issues related to ultrasound acquisition described above, such as image resolution, may affect *in vivo* evaluation of DMC liner orientation.

The post processing experiments performed here concerned specific static positions. A valuable extension for future research would be to apply this method to dynamic situations. However, while the ultrafast option is available for

ultrasound acquisitions, it would be challenging to maintain contact between the ultrasound probe and the groin area during the patient movements involved in daily-life activities.

5. Conclusion

This work validates the feasibility and assesses the accuracy and precision of a method based on ultrasound imaging to analyse the liner orientation of submerged DMC-THA and implanted DMC-THA *ex vivo*. The research should be extended by performing *in vivo* experiments to visualise and quantify liner movement after different hip movements. Liner movement can be computed relative to the pelvis coordinate system, obtained in this case from skin markers placed on the anterior and posterior iliac spines. Both *ex vivo* experiments [15] and *in vivo* measurements using ultrasound imaging [14] have previously shown that the liner is affected by iliopsoas tendon impingement. Thus, this work opens new possibilities to observe the possible contact between liner and iliopsoas tendon during patient movements, using ultrasound imaging, which should improve clinical understanding of liner movement in DMC-THA.

Authors' contributions

All authors contributed to the conception and design of the study and to manuscript revision, and all read and approved the submitted version. LR, AN, AV, TDL and L-LG performed the experiments and collected and treated raw data (ultrasound and motion analysis). LR, AN, HL, RD and L-LG analysed and discussed the data. LR, AN, HL, RD and L-LG wrote the first draft of the manuscript.

Ethical approval

Ethics approval was not required for this study since it is not required by French law.

Acknowledgments

The authors thank Leïla Ben Boubaker for her help in carrying out experiments.

The authors thank the Serf company for lending prostheses and materials for the implantation.

Funding

This work was supported by the LABEX PRIMES (ANR-11-LABX-0063) of Université de Lyon, within the program "Investissements d'Avenir" (ANR-11-IDEX-0007) operated by the French National Research Agency (ANR).

Declaration of Competing Interest

AV is a consultant for Serf and Smith & Nephew and M-HF receives royalties from Serf and DePuy. LR, AN, TDL, HL, RD, and L-LG declare no conflict of interest.

References

[1] Batailler C, Fary C, Verdier R, Aslanian T, Caton J, Lustig S. The evolution of outcomes and indications for the dual-mobility cup: a systematic review. International Orthopaedics (SICOT) 2017;41:645–59. https://doi.org/10.1007/s00264-016-3377-y.

[2] Berry DJ, von Knoch M, Schleck CD, Harmsen SW. The Cumulative Long-Term Risk of Dislocation After Primary Charnley Total Hip Arthroplasty: The Journal of Bone and Joint Surgery-American Volume 2004;86A:9–14. https://doi.org/10.2106/00004623-200401000-00003.

[3] Bozic KJ, Kurtz SM, Lau E, Ong K, Vail TP, Berry DJ. The Epidemiology of Revision Total Hip Arthroplasty in the United States. The Journal of Bone & Joint Surgery 2009;91:128–33.

[4] Noyer D, Caton JH. Once upon a time.... Dual mobility: history. International Orthopaedics (SICOT) 2017;41:611–8. https://doi.org/10.1007/s00264-016-3361-6.

[5] Charnley J. Total Hip Replacement by Low-Friction Arthroplasty. Clinical Orthopaedics and Related Research (1976-2007) 1970;72:7–21.

[6] Neri T, Boyer B, Batailler C, Klasan A, Lustig S, Philippot R, et al. Dual mobility cups for total hip arthroplasty: tips and tricks. SICOT-J 2020;6:17. https://doi.org/10.1051/sicotj/2020018.

[7] Darrith B, Courtney PM, Della Valle CJ. Outcomes of dual mobility components in total hip arthroplasty: a systematic review of the literature. The Bone & Joint Journal 2018;100-B:11–9. https://doi.org/10.1302/0301-620X.100B1.BJJ-2017-0462.R1.

[8] Fessy M-H, Jacquot L, Rollier J-C, Chouteau J, Ait-Si-Selmi T, Bothorel H, et al. Midterm Clinical and Radiographic Outcomes of a Contemporary Monoblock Dual-Mobility Cup in Uncemented Total Hip Arthroplasty. The Journal of Arthroplasty 2019;34:2983–91. https://doi.org/10.1016/j.arth.2019.07.026.

[9] Assi C, El-Najjar E, Samaha C, Yammine K. Outcomes of dual mobility cups in a young Middle Eastern population and its influence on life style. International Orthopaedics (SICOT) 2017;41:619–24. https://doi.org/10.1007/s00264-016-3390-1.

[10] Rowan FE, Salvatore AJ, Lange JK, Westrich GH. Dual-Mobility vs Fixed-Bearing Total Hip Arthroplasty in Patients Under 55 Years of Age: A Single-Institution, Matched-Cohort Analysis. The Journal of Arthroplasty 2017;32:3076–81. https://doi.org/10.1016/j.arth.2017.05.004.

[11] Terrier A, Latypova A, Guillemin M, Parvex V, Guyen O. Dual mobility cups provide biomechanical advantages in situations at risk for dislocation: a finite element analysis. International Orthopaedics (SICOT) 2017;41:551–6. https://doi.org/10.1007/s00264-016-3368-z.

[12] Fessy MH, Riglet L, Gras L-L, Neyra H, Pialat J-B, Viste A. Ilio-psoas impingement with a dual-mobility liner: an original case report and review of literature. SICOT-J 2020;6:27. https://doi.org/10.1051/sicotj/2020025.

[13] Nebergall AK, Freiberg AA, Greene ME, Malchau H, Muratoglu O, Rowell S, et al. Analysis of Dual Mobility Liner Rim Damage Using Retrieved Components and Cadaver Models. The Journal of Arthroplasty 2016;31:1595–602. https://doi.org/10.1016/j.arth.2015.12.032.

[14] Layton RB, Messenger N, Stewart TD. Analysis of hip joint cross-shear under variable activities using a novel virtual joint model within Visual3D. Proc Inst Mech Eng H 2021;235:1197–204. https://doi.org/10.1177/09544119211025869.

[15] Calonius O, Saikko V. Slide track analysis of eight contemporary hip simulator designs. Journal of Biomechanics 2002;35:1439–50. https://doi.org/10.1016/S0021-9290(02)00171-9.

[16] Fessy M-H, Huten D. La double mobilité en marche dans les prothèses totales de hanche. Elsevier Masson; 2018.

[17] Gao Y, Zhao X, Chen S, Zhang J, Chen Z, Jin Z. Effects of Daily Activities and Position on Kinematics and Contact Mechanics of Dual Mobility Hip Implant. Journal of Healthcare Engineering 2020;2020:1–12. https://doi.org/10.1155/2020/8103523.

[18] Vahedi H, Makhdom AM, Parvizi J. Dual mobility acetabular cup for total hip arthroplasty: use with caution. Expert Review of Medical Devices 2017;14:237–43. https://doi.org/10.1080/17434440.2017.1292123.

[19] Fabry C, Kaehler M, Herrmann S, Woernle C, Bader R. Dynamic behavior of tripolar hip endoprostheses under physiological conditions and their effect on stability. Medical Engineering & Physics 2014;36:65–71. https://doi.org/10.1016/j.medengphy.2013.09.007.

[20] Varadarajan KM, Zumbrunn T, Duffy MP, Patel R, Freiberg AA, Rubash HE, et al. Reducing the distal profile of dual mobility liners can mitigate soft-tissue impingement and liner entrapment without affecting mechanical performance: CONTOURED DUAL MOBILITY LINER. J Orthop Res 2016;34:889–97. https://doi.org/10.1002/jor.23078.

[21] Zumbrunn T, Patel R, Duffy MP, Rubash HE, Malchau H, Freiberg AA, et al. Cadaver-Specific Models for Finite-Element Analysis of Iliopsoas Impingement in Dual-Mobility Hip Implants. The Journal of Arthroplasty 2018;33:3574–80. https://doi.org/10.1016/j.arth.2018.06.029.

[22] Desmarchelier R, Gras L-L, Fessy M-H. Validation d'une méthode échographique du suivi du comportement biomécanique d'une PTH double mobilité. Revue de Chirurgie Orthopédique et Traumatologique 2016;102:S179. https://doi.org/10.1016/j.rcot.2016.08.247.

[23] Desmarchelier R, Gras L-L, Viste A, Fessy M-H. Analyse in vivo de la mobilité du polyéthylène par échographie : perspectives. La double mobilité en marche dans les prothèses totales de hanche. Elsevier Masson, 2018, p. 67–71.

[24] Besl PJ, McKay ND. A method for registration of 3-D shapes. IEEE Trans Pattern Anal Mach Intell 1992;14:239–56. https://doi.org/10.1109/34.121791.

[25] Riglet L, Viste A, Dumas R, Liebgott H, Fessy MH, Gras L-L. Geometric reconstruction of a dual mobility cup liner using ultrasound imaging. Computer Methods in Biomechanics and Biomedical Engineering 2021;24:pp S295-S297. https://doi.org/10.1080/10255842.2021.1978758.

[26] Wu G, Siegler S, Allard P, Kirtley C, Leardini A, Rosenbaum D, et al. ISB recommendation on definitions of joint coordinate system of various joints for the reporting of human joint motion—part I: ankle, hip, and spine. Journal of Biomechanics 2002;35:543–8. https://doi.org/10.1016/S0021-9290(01)00222-6.

[27] Derrick TR, van den Bogert AJ, Cereatti A, Dumas R, Fantozzi S, Leardini A. ISB recommendations on the reporting of intersegmental forces and moments during human motion analysis. Journal of Biomechanics 2020;99:109533. https://doi.org/10.1016/j.jbiomech.2019.109533.

[28] Biedermann R, Krismer M, Stöckl B, Mayrhofer P, Ornstein E, Franzén H. Accuracy of EBRA-FCA in the measurement of migration of femoral components of total hip replacement. THE JOURNAL OF BONE AND JOINT SURGERY 1999;81:7.

[29] Nunn D, Freeman M, Hill P, Evans S. The measurement of migration of the acetabular component of hip prostheses. The Journal of Bone and Joint Surgery British Volume 1989;71-B:629–31. https://doi.org/10.1302/0301-620X.71B4.2768311.

[30] Jørgensen PB, KAPTEIN BL, SØBALLE K, JAKOBSEN SS, STILLING M. Polyethylene liner motion in dual-mobility hip prostheses: static and dynamic radiostereometry in 16 patients 1 year after operation. Acta Orthop 2022;93:375–81. https://doi.org/10.2340/17453674.2022.2253.

[31] Moore MS, McAuley JP, Young AM, Engh CA. Radiographic Signs of Osseointegration in Porous-coated Acetabular Components. Clinical Orthopaedics & Related Research 2006;444:176–83. https://doi.org/10.1097/01.blo.0000201149.14078.50.

[32] Massin P, Schmidt L, Engh CA. Evaluation of cementless acetabular component migration: An experimental study. The Journal of Arthroplasty 1989;4:245–51. https://doi.org/10.1016/S0883-5403(89)80020-8.

[33] Elke R, Berli B, Wagner A, Morscher EW. Acetabular revision in total hip replacement with a press-fit cup. THE JOURNAL OF BONE AND JOINT SURGERY 2003;85:6.

[34] Lachiewicz PF, Poon ED. Revision of a Total Hip Arthroplasty with a Harris-Galante Porous-Coated Acetabular Component Inserted without Cement. A Follow-up Note on the Results at Five to Twelve Years*. JBJS 1998;80:980–4.

[35] Szabo TL. Diagnostic ultrasound imaging: inside out. Amsterdam ; Boston: Elsevier Academic Press; 2004.

[36] Vray D, Brusseau E, Detti V, Varray F, Basarab A, Beuf O, et al. Ultrasound Medical Imaging. Medical Imaging Based on Magnetic Fields and Ultrasounds, John Wiley & Sons, Ltd; 2014, p. 1–72. https://doi.org/10.1002/9781118761236.ch1.

[37] Fantino O, Tayot O, Sans N, Cyteval C. Imagerie des prothèses totales de hanche : aspect normal et pathologique, place de l'échographie, du scanner et de l'IRM. Journal de Radiologie 2011;92:594–620. https://doi.org/10.1016/j.jradio.2011.04.007.

[38] Lewinnek et al. Dislocation after Total Hip-Replacement Arthroplasties. The Journal of Bone and Joint Surgery 1978;60-A:217–20.

[39] Noble JA. Ultrasound image segmentation and tissue characterization. Proc Inst Mech Eng H 2010;224:307–16. https://doi.org/10.1243/09544119JEIM604.

[40] Noble JA, Boukerroui D. Ultrasound image segmentation: a survey. IEEE Trans Med Imaging 2006;25:987–1010. https://doi.org/10.1109/TMI.2006.877092.

[41] Brattain LJ, Telfer BA, Dhyani M, Grajo JR, Samir AE. Machine learning for medical ultrasound: status, methods, and future opportunities. Abdom Radiol 2018;43:786–99. https://doi.org/10.1007/s00261-018-1517-0.

[42] Liu S, Wang Y, Yang X, Lei B, Liu L, Li SX, et al. Deep Learning in Medical Ultrasound Analysis: A Review. Engineering 2019;5:261–75. https://doi.org/10.1016/j.eng.2018.11.020.

[43] Klemt C, Bounajem G, Tirumala V, Xiong L, Padmanabha A, Kwon Y. Three- dimensional kinematic analysis of dislocation mechanism in dual mobility total hip arthroplasty constructs. J Orthop Res 2020:jor.24855. https://doi.org/10.1002/jor.24855.

[44] Boyer B, Philippot R, Geringer J, Farizon F. Primary total hip arthroplasty with dual mobility socket to prevent dislocation: a 22-year follow-up of 240 hips. International Orthopaedics (SICOT) 2012;36:511–8. https://doi.org/10.1007/s00264-011-1289-4.

[45] Vielpeau C, Lebel B, Ardouin L, Burdin G, Lautridou C. The dual mobility socket concept: experience with 668 cases. International Orthopaedics (SICOT) 2011;35:225–30. https://doi.org/10.1007/s00264-010-1156-8.

Table 1. PMHS anatomic and arthroplasty information.

Subject	Age Years	Sex Male/Female	Weight (kg)	Height (cm)	Head Diameter (mm)	Liner Diameter Right/Left (mm)	Acetabular Cup Diameter Left/Right (mm)
2020 191	78	M	102	177	28	NA/47	NA/53
2021 29	105	F	41	150	28	43/NA	49/NA
2021 48	93	F	46	156	28	43/43	49/49
2021 107	82	F	56	157	28	43/43	49/49

Table 2. Ultrasound acquisition procedure repeatability and intra-operator segmentation repeatability of abduction and anteversion angle of the liner plane for cadaveric subjects. Ultrasound acquisition procedure repeatability was not calculated for subject 2020_191_L. Range is the difference between minimum and maximum angle obtained by

segmentation. Repeatability is measured for different liner positions but with the same subject's position (straight leg with no internal/external rotation).

			2020 191 L	2021 29 R	2021 48 L	2020 48 R	2020 107 L	2021 107 R
			Angle (°)	*Angle (°)*	*Angle (°)*	*Angle (°)*	*Angle (°)*	*Angle (°)*
Ultrasound acquisition procedure repeatability	**Mean**	*Abduction*	-	71.3	60.2	67.1	31.5	54.9
		Anteversion	-	3.5	10.6	11.5	30.5	15.6
	SD	*Abduction*	-	1.0	1.3	0.9	0.7	1.0
		Anteversion	-	0.9	1.3	0.8	1.1	0.9
	Range	*Abduction*	-	2.6	3.4	2.4	1.6	3.3
		Anteversion	-	2.6	2.6	1.9	2.7	2.3
Intra-operator segmentation repeatability	**Mean**	*Abduction*	66.6	80.8	51.4	53.7	67.4	41.1
		Anteversion	1.9	12.1	11.8	-7.3	20.5	33.4
	SD	*Abduction*	0.7	0.7	0.7	0.7	0.3	0.6
		Anteversion	0.7	1.3	0.7	0.9	0.5	0.3
	Range	*Abduction*	1.9	2.2	1.8	2.0	1.0	1.7
		Anteversion	1.9	2.9	1.9	2.0	1.5	0.9

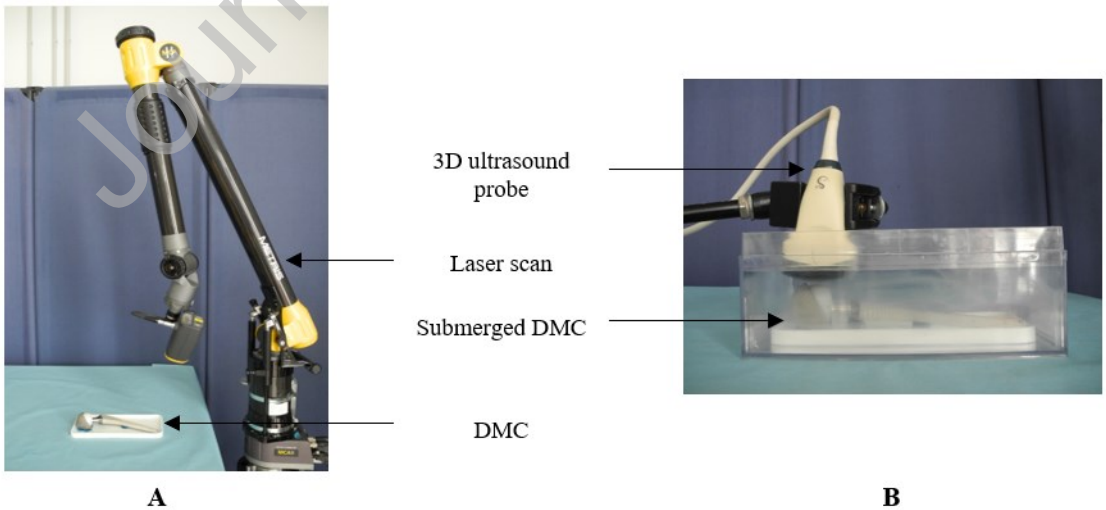

Figure 1. A - 3D laser scan setup for dry DMC-THA. B – Ultrasound setup for submerged DMC-THA.

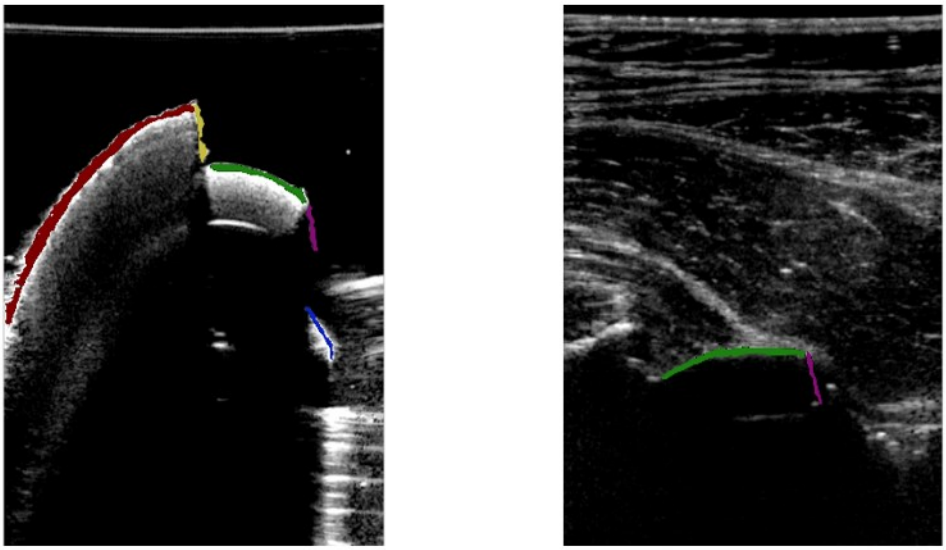

A B

Figure 2. Ultrasound images of the dual mobility cup: submerged (A) and implanted (B), and representation of all segmented elements: red = cup ; yellow = cup plane ; green = liner ; magenta = liner plane ; blue = head. The reader can refer to the online version of the article for a coloured version of the figure.

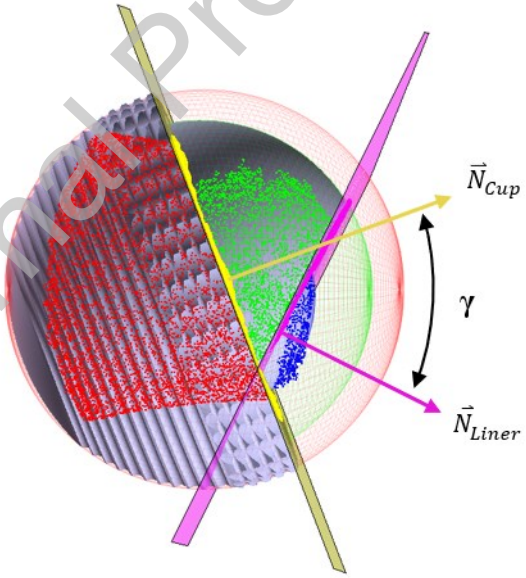

Figure 1. 3D ultrasound process for the submerged dual mobility cup. Red dots and sphere = cup ; yellow dots, plane and normal = cup plane ; green dots and sphere = liner ; magenta dots, plane and normal = liner plane ; blue dots and sphere = head ; grey = implant CAD models ; γ = angle between cup plane and liner plane. The reader can refer to the online version of the article for a coloured version of the figure

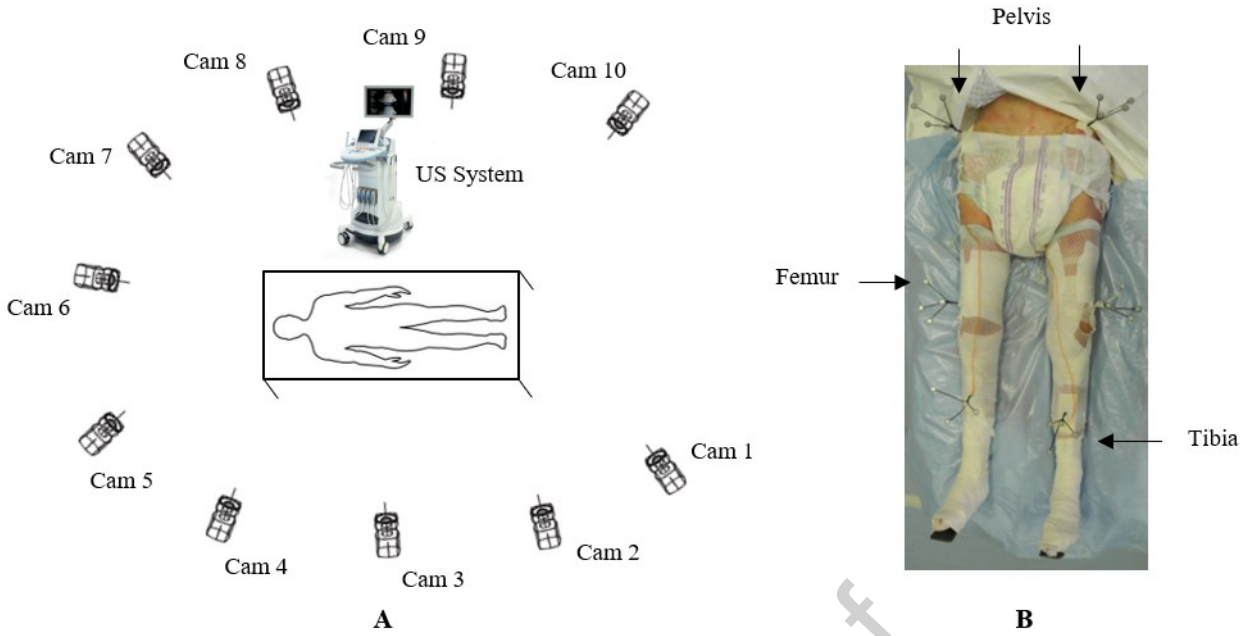

Figure 4. A – Motion analysis system with 10 cameras and ultrasound imaging system positions in experimental area. B – Intracortical pins (tripods with reflective markers) for motion analysis fixed in pelvis, femur and tibia

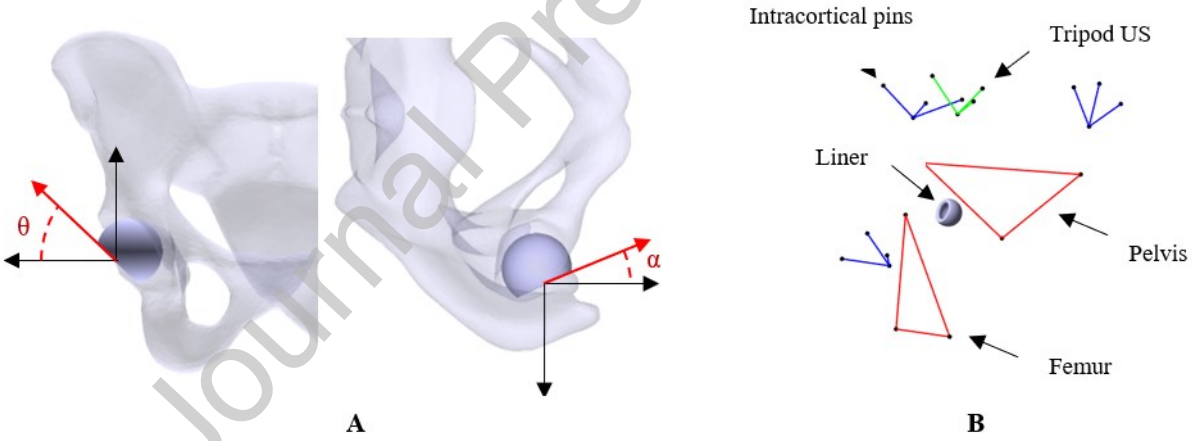

Figure 5. A – Liner abduction (θ) and anteversion (α). B – Liner position using ultrasound and motion analysis data